CHEMICAL ENGINEERING TRANSACTIONS
VOL. 46, 2015
A publication of AIDIC
The Italian Association of Chemical Engineering
Online at www.aidic.it/cet
Guest Editors: Peiyu Ren, Yancang Li, Huiping Song

ISBN 978-88-95608-37-2; **ISSN** 2283-9216
DOI: 10.3303/CET1546153

Performance of Brillouin Optical Time Domain Reflectometry with a Reference Brillouin Ring Laser

Rugang Wang*[a, b], Feng Zhou[a] and Li Zhao[b]

[a] School of Information Technology, Yancheng Institute of Technology, Yancheng 224051, China,
[b] School of Information Science and Engineering, Southeast University, Nanjing, 210096, China.
wrg3506@ycit.edu.cn

A Brillouin optical time domain reflectometry (BOTDR) with the reference Brillouin laser for distributed measurement over long range fiber is experimentally demonstrated. A passive configuration using Mach-Zehnder interferometer is used to eliminate the polarization noise in the BOTDR. Experimental results show that the new system can effectively reduce the polarization noise. The Brillouin frequency shift induced by heated can be accurately detected by the BOTDR over 53km, and the temperature measurement error is less than 1.0^0C.

1. Introduction

Brillouin optical time domain reflectometry (BOTDR) is capable of measuring strain and temperature over a long range sensing, Feng Wang et al (2012) and Rugang Wang et al (2014) reported the BOTDR is particularly import in structural health monitoring. The spontaneous Brillouin scattering is very weak, Yougang Sun et al (2014) reported the heterodyne detection technique is used to detect the weak signal because it offers much high sensitivity and dynamic range. If the pump laser is used as a local oscillator (LO) in BOTDR system, the beat signal is around 11GHz, which requires an over 11GHz bandwidth detector , which was confirmed by T. Horiguchi et al (1995). However, a wider bandwidth detector has higher noise equivalent power (NEP), which would reduce the measuring strain and temperature accuracy. To avoid using wide bandwidth electronics, several approaches have been proposed for heterodyne detection in BOTDR, such as the modulation technique with optical modulator, which was confirmed by S. B. Cho et al (2004) and V. Lantich et al (2009), the Brillouin fiber laser, which was confirmed by V. Lecoeuche et al (1998) and J. Geng et al (2007), and so on. In modulation technique the high-speed modulator driven by a microwave source must be used. The modulator has to be precisely controlled in this method, and the high-order sideband components induced in process of modulation make the signal analysis more complex due to signal interferences between those high-order components and Brillouin scattering light. The method using a Brillouin fiber laser as local light for heterodyne detection has also received great attention. However, most of the reported schemes for obtaining the Brillouin fiber laser require specially designed configuration with high speed modulator, lock-in amplifier or selective gate, which would make the system very complicated and costly. These complicated and costly features are major factors that discourage the wide-spread use of BOTDR systems.
In this paper, a stabilized single frequency Brillouin fiber laser is experimentally demonstrated without using expensive instruments or complicated system. And a passive configuration using Mach-Zehnder interferometer is used to eliminate the polarization noise in the BOTDR. A BOTDR for distributed measurement over long range sensing fiber has been developed using the reference Brillouin laser.

2. Experimental Setup

The experimental setup is shown in Fig. 1. The output lightwave of the laser is divided into two beams with a 95/5 polarization-maintaining (PM) coupler (coupler 1). The 95% port is modulated into the probe pulse by two electro-optic modulators (EOMs) driven by a pulse generator to get a high extinction ratio. A polarization controller (PC) PC1 is inserted between EOM1 and EOM2 to optimize the polarization state of the input lightwave for EOM2, the probe pulse is amplified by an Erbium doped fiber amplifier (EDFA) EDFA 1 and then

Please cite this article as: Wang R.G., Zhou F., Zhao L., 2015, Performance of brillouin optical time domain reflectometry with a reference brillouin ring laser, Chemical Engineering Transactions, 46, 913-918 DOI:10.3303/CET1546153

the lightwave is injected into the polarization depolarizer scheme shown in the dashed rectangular in Fig. 1. The linewidth of the lightwave in our system is 700 KHz, so its coherence length is less than 100 m. A single mode fiber (SMF) SMF 1 with 5km length is inserted into one arm between PBS1 and PBS2 as a delay fiber. The PC2 is used into other arm between PBS1 and PBS2. After passing through this scheme, the probe pulse is injected into the sensing fiber through a circulator (OC) OC1. The spontaneous Brillouin scattering induced by the probe pulse will propagates back to the 50/50 coupler (coupler 3) in front of the balanced photo-detector (PD). The local oscillator light of the heterodyne detection for BOTDR is a fiber Brillouin ring laser, which consists of OC2, PC, isolator (ISO) ISO2, SMF2 and 80/20 coupler (coupler 2). Another beam from coupler1 is sent into the ring Brillouin laser via OC2 after amplified by an EDFA2. To make sure that the first-order Stokes light excited in the cavity, the ISO2 is used at the propagation direction of the first-order Stokes light. The spontaneous Brillouin scattering induced by the probe pulse from the sensing fiber is measured by heterodyning the output of Brillouin laser from the 20% port of coupler 2 with the backscattered light on a balanced PD. The electrical spectrum analyzer (ESA) and the signal processing system are used to process the electrical signal.

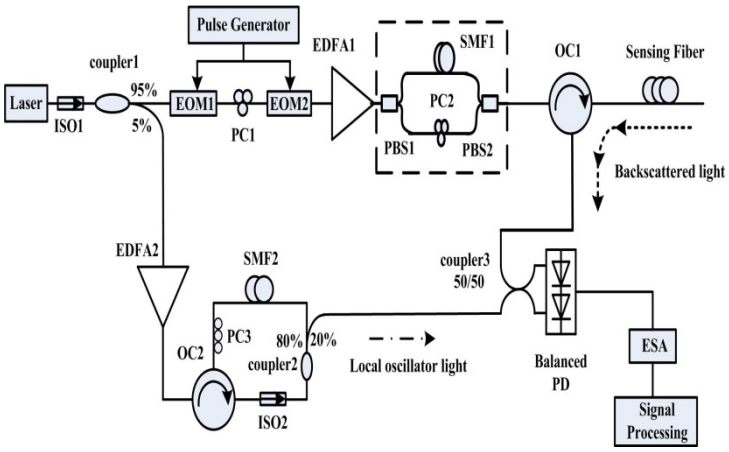

Figure. 1 Experimental setup of BOTDR

3. Results and Discussion

The mode spacing of the fiber ring laser is determined by the cavity length, and the measured mode spacing of the Brillouin laser is shown in Fig. 2. It can be seen that the mode spacing in Fig. 2 is 18MHz, which is consistent with 11m long cavity, the extinction ratio between the modes is 18dB and this mode spacing can operate in single frequency due to the mode competition between modes, which was confirmed by D. Lida et al (2009) and A. Debut et al (2001). The heterodyne detection BOTDR with this single frequency local light would have high stability on frequency due to the single frequency local light.

A passive scheme based on Mach-Zehnder interference is proposed to eliminate the polarization noise in BOTDR. Its configuration is shown in dashed box in Fig. 1 which is mainly composed of two polarization beam splitters (PBS's). The angle of incidence for PBS1 is 45°. When a linearly polarized light paralleling to one of the axes of polarization-maintaining (PM) fiber is input into PBS1, it will be split into two beams equally whose polarization directions are orthogonal to each other. These two beams are coupled into two output arms of PBS1 respectively and then are combined together through PBS2 which is used as a polarization beam combiner. A PM fiber whose length is much longer than the coherent length of the input beam is inserted into one output arm of PBS1. By using this scheme, we can obtain a reference beam composed of two orthogonal beams with equal power, and their phase relationship changes randomly. The linewidth of the lightwave in our system is 500 KHz, so its coherence length is less than 100 m. A single mode fiber (SMF) SMF 1 with 5km length is inserted into one arm between PBS1 and PBS2 as a delay fiber. The PC2 is used into other arm between PBS1 and PBS2. In addition, the power of the output beam equals to the power of the input beam theoretically by using such a scheme. The pulse width of the probe optical pulse is 50ns. Its peak power is 22dBm before the OC1. The length of the sensing fiber is about 50km and the power of the reference lightwave out from the Brillouin ring laser is 3.0 dBm. After 2000 averages, the spatial distribution of Brillouin scattering signal along the fiber with and without the polarization depolarizer are shown respectively in Fig. 3. Apparently, the polarization noise in BOTDR is eliminated significantly by the polarization depolarizer, and the polarization noise is only 4% with the polarization depolarizer than that without it.

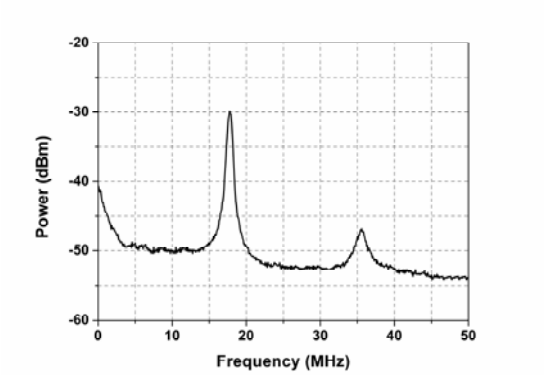

Figure. 2 The mode spacing of the Brillouin laser

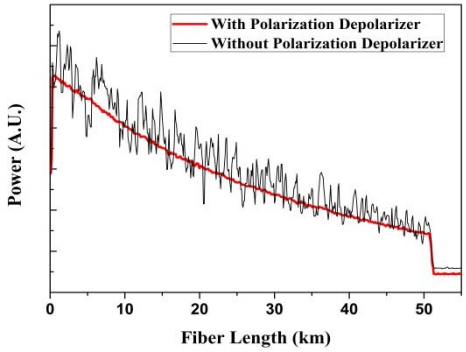

Figure. 3 Spatial distribution of Brillouin scattering signal along the fiber

The structure of sensing fiber is shown in Fig. 4 and it consists of SMF1, SMF2, SMF3 and SMF4. The length of SMF1+SMF2, SMF3 and SMF4 is 9765m, 35m and 220m, respectively. The SMF3 is heated to 85^0C and the room temperature is 29^0C. After 2000 times average, the spatial distribution of Brillouin scattering signal along the fiber for 50ns and 100ns probe pulse are shown in Fig. 5. The electrical signal from the PD was measured using an ESA operated in zero scan modes to allow the collection of time domain traces. It can be seen that the intensity of Brillouin scattering signal decays exponentially along the sensing fiber. According to the relationship between Brillouin frequency shift and temperature, the changes of the Brillouin frequency shift of the SMF3 in the oven is obviously observed and shown as (A) in Fig. 5. The Brillouin frequency shift of SMF1 and SMF2 are different, there is a Brillouin scattering spectrum of SMF2 shown as (B) in Fig. 5. The distribution of Brillouin frequency shift along the sensing fiber is shown in Fig. 6. It can be seen that the Brillouin frequency shifts of the unheated fiber are 10.917GHz. The Brillouin frequency shifts of SMF3 at 60^0C, 70^0C and 85^0C are 10.945, 10.955 and 10.971GHz for 50ns or 100ns pulse, respectively. The Brillouin frequency shift differences are 10MHz and 16MHz. The differences of Brillouin frequency shifts are proportional to the temperature of SMF3 with 1MHz/^{0}C slope, which is in excellent agreement with the literature Zhong Qiu-bo et al (2015) and Dong Mian et al (2014). It can be seen that the length of heated fiber (SMF3) in the inset of the Fig. 6 is 35m, and the spatial resolution at 50ns and 100ns is 5m and 10m, respectively. The Brillouin frequency shift of SMF2 shown as (C) in Fig. 6 is coincident with the Brillouin spectrum shown as (B) in Fig. 5.

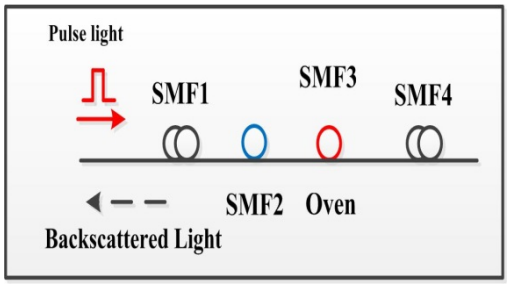

Figure. 4 Structure of sensing fiber

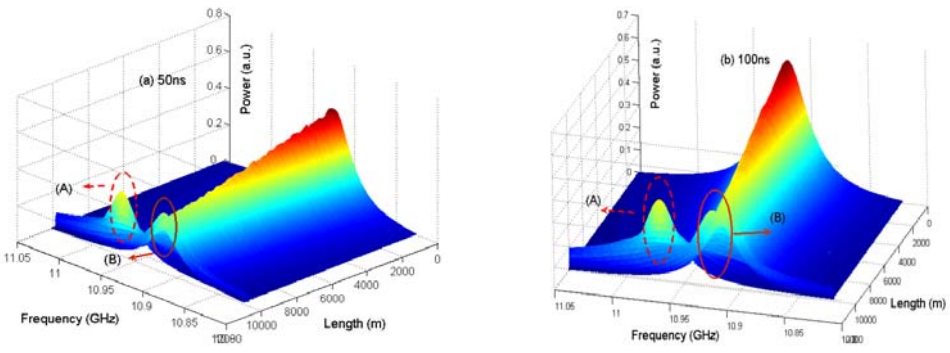

(a) (b)

Figure. 5 Spatial distribution of Brillouin scattering signal along the fiber (a) 50ns pulse width. (b) 100ns pulse width

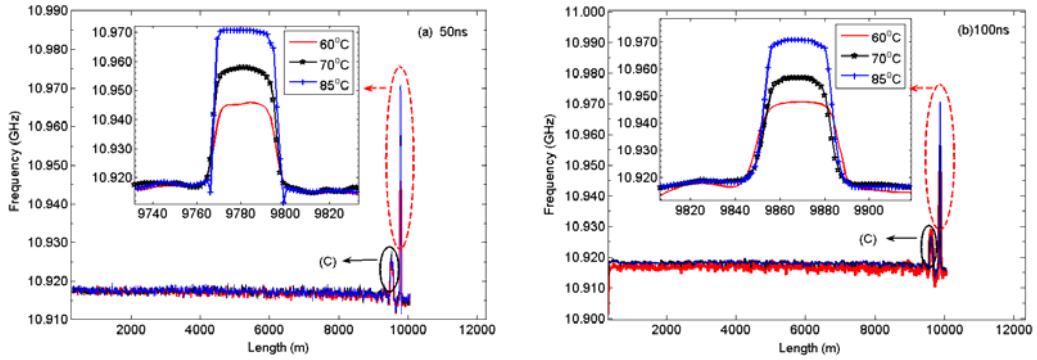

(a) (b)

Figure. 6 The distribution of Brillouin frequency shift along the fiber. (a) 50ns pulse width, (b) 100ns pulse width

To further evaluate the performance of the BOTDR using the novel Brillouin fiber laser, the SMF3 is heated at temperature of 60^0C, 70^0C and 85^0C by an oven. Fig. 7 shows the spectra of SMF3 at different temperature after Lorentz fit with 50ns and 100ns pulse width. The Brillouin spectral widths for pulse widths of 50ns and 100ns are about 39MHz and 37MHz, respectively, which is mainly attributed to the difference of the pulse spectrum, and this is also commonly observed with conventional BOTDR [12]. It can be seen that the difference of the Brillouin frequency shift at different temperature is clearly distinguished. The Brillouin frequency shift of SMF3 at the reference temperature is about 10.917GHz, and the Brillouin frequency shift of SMF3 at 60^0C, 70^0C and 85^0C is about 10.945, 10.955 and 10.971GHz, respectively. There are few differences of Brillouin frequency shift for 50ns and 100ns pulse width. The Brillouin frequency shift distribution can be obtained and the heated section is successfully identified by using the Lorentz fit the Brillouin spectrum along the fiber as shown in Fig. 7. It can also be seen that the Brillouin frequency shifts of the unheated are 10.917GHz, and the Brillouin frequency shift of SMF3 at 60^0C, 70^0C and 85^0C is about 10.945, 10.955 and 10.971GHz for 50ns or 100ns pulse, respectively. Their difference is about 10MHz and 16MHz, and the temperature measurement error is less than 1.0^0C. The difference of Brillouin frequency shifts is proportional to the temperature of SMF3 with 1MHz/^{0}C slope, which is in excellent agreement with the literature [13]. We can see that the length of heated fiber (SMF3) in the inset of the Fig. 6 is about 35m, and the spatial resolution at 50ns and 100ns is about 5m and 10m, respectively. The position (C) in Fig. 6 is the Brillouin frequency shift of SMF2, which is agree with the position (B) in Fig. 5.

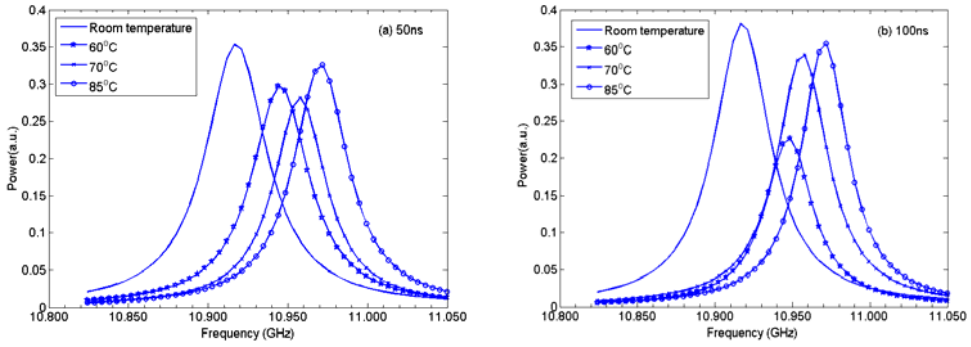

(a) (b)

Figure. 7 Brillouin spectra of SMF3 with 50ns and 100ns pulse width, (a) 50ns, (b) 100ns

The spatial distribution of Brillouin scattering signal along the 53km sensing fiber are shown in Fig. 8. The length of SMF1+SMF2, SMF3 and SMF4 is 48.63km, 123m and 4.823km, respectively. The heated section of the fiber can be clearly seen and the dynamic range is 0.5dB shown in Fig. 8 (a). And the intensity of Brillouin scattering signal decays exponentially along the sensing fiber. The measured Brillouin frequency shift of SMF1 and SMF4 is 10.911GHz and 10.903GHz. The measured Brillouin frequency shift of SMF3 at 70^{0}C and 85^{0}C is 10.742GHz and 10.958GHz respectively, and the frequency difference is 16MHz. It should be noted that, although the measurement temperature error is somewhat high, it can be further improved by controlling the temperature of the SMF5 in the Brillouin laser and the method of fit.

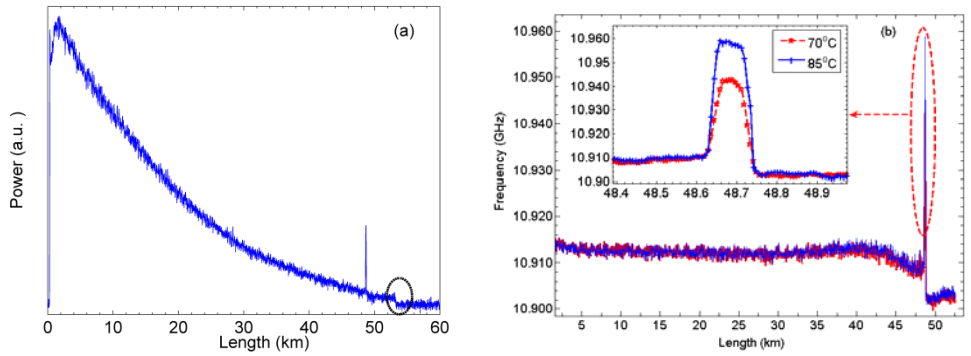

(a) (b)

Figure. 8 Distribution of Brillouin scattering signal along the fiber. (a) Distribution of Brillouin scattering power along the fiber at 10.951GHz Brillouin frequency shift. (b) Distribution of Brillouin frequency shift along the fiber

4. Conclusion

In this paper, a BOTDR with the reference Brillouin laser for distributed measurement over long range fiber is experimentally demonstrated. A passive configuration using Mach-Zehnder interferometer is used to eliminate the polarization noise in the BOTDR. Experimental results show that the new system can effectively reduce the polarization noise. The Brillouin frequency shift induced by heated can be accurately detected by the BOTDR over 53km, and the temperature measurement error is less than 1.0^{0}C.

Acknowledgements

This work is supported by China Postdoctoral Science Foundation under contracts No. 2015M571637, the Colleges and Universities Natural Science Foundation in Jiangsu Province under contracts No. 14KJB510034, and the Talent introduction project of Yancheng Institute of Technology No. KJC2013014.

References

Cho S.B., and Lee J.J., 2004, Strain event detection using a double-pulse technique of a Brillouin scattering-based distributed optical fiber sensor. Opt. Express, 12 (18): 4339-4346, DOI: 10.1364/OPEX.12.004339.

Debut A., Randoux S., and Zemmouri J., 2001, Experimental and theoretical study of linewidth narrowing in Brillouin fiber ring lasers. J. Opt. Soc. Am. B, 18 (4): 556-567, DOI: 10.1364/JOSAB. 18.000556.

Geng J., Staines S., Blake M., and Jiang S., 2007, Distributed fiber temperature and strain sensor using coherent radio-frequency detection of spontaneous Brillouin scattering. Applied Optics, 46 (23): 5928-5932, DOI: 10.1364/AO.46.005928.

Guo M.M., Yang S.L., Yan H., Kan L.F. and Yang B., 2014, Mobile video alarm system based on cloud computing. Review of Computer Engineering Studies, 2014, 1 (2): 5-10 DOI: 10.18280/rces.010202

Horiguchi T., Shimizu K., Kurashima T., Tateda M., and Koyamada Y., 1995, Development of a distributed sensing technique using Brillouin scattering. J. Lightwave Technol., 13 (7): 1296-1302, DOI: 10.1109/50.400684.

Lanticq V., Jiang S., Gabet R., Jaouen Y., Taillade F., Moreau G., and Agrawal G.P., 2009, Self-referenced and single-ended method to measure Brillouin gain in monomode optical fibers. Opt. Lett., 34 (7): 1018-1020, DOI: 10.1364/OL.34.001018.

Lecoeuche V., Webb D.J., Pannellm C.N., Jackson D.A., 1998, Brillouin based distributed fiber sensor incorporating a mode-locked Brillouin fiber ring laser. Optics. Comm., 152: 263-268, DOI: 10.1016/S0030-4018(98)00187-4.

Lida D., and Ito F., 2009, Cost-effective bandwidth-reduced Brillouin optical time domain reflectometry using a reference Brillouin scattering beam. Applied Optics, 48 (22): 4302-4309 DOI: 10.1364/AO.48.004302.

Maughan S.M., Kee H.H., and Newson T.P., 2001, A calibrated 27km distributed fiber temperature sensor based on microwave heterodyne detection of spontaneous Brillouin scattered power. IEEE Photon. Technol. Lett., 13 (5): 511-513, DOI: 10.1109/68.920769.

Mian D., Gang S.Y., Qing H.Y. and Wei X.T., 2014, Modeling and simulation research of active heave compensation system. Review of Computer Engineering Studies, 1 (2): 15-18 DOI: 10.18280/rces.010204

Sun Y.G., Qiang H.Y., Yang K.R., Chen Q.L., Dai G.W., Dong M., 2014, Experimental design and development of heave compensation system for marine crane. Mathematical modeling and Engineering Problems, 1 (2): 15-22. DOI: 10.18280/mmep.01020

Wang F., Li C.L., Zhao X.D., and Zhang X.P., 2012, Using a Mach-Zehnder-interference-based passive configuration to eliminate the polarization noise in Brillouin optical time domain reflectometry. Applied Optics, 51 (2): 176-180 DOI: 10.1364/AO.51.000176.

Wang R.G., Zhou L.Y., 2014, Performance of Brillouin optical time domain reflectometer with erbium doped fiber amplifier [J]. Optik, 125 (17): 4864-4867, DOI:10.1016/j.ijleo. 2014.04.040.

Wan S.P., Xiong Y.H., and He X.D., 2014, The theoretical analysis and design of coding BOTDR system with APD detector. IEEE sensor journal, 14 (8): 2626-2632, DOI: 10.1109/JSEN. 2014.2310141.

Zhong Q.B., Zhao J., Tong C.Y., 2015, Design and implement of entertainment and competition humanoid robot. Review of Computer Engineering Studies, 2015, 2 (1): 15-22. DOI: 10.18280/rces.020103